

Soliton Solution, Bäcklund Transformation, and Conservation Laws for the Sasa-Satsuma Equation in the Optical Fiber Communications

Ying Liu^a, Yi-Tian Gao^{a,b}, Tao Xu^c, Xing Lü^c, Zhi-Yuan Sun^a, Xiang-Hua Meng^c, Xin Yu^a, and Xiao-Ling Gai^a

^a Ministry-of-Education Key Laboratory of Fluid Mechanics and National Laboratory for Computational Fluid Dynamics, Beijing University of Aeronautics and Astronautics, Beijing 100191, China

^b State Key Laboratory of Software Development Environment, Beijing University of Aeronautics and Astronautics, Beijing 100191, China

^c School of Science, P. O. Box 122, Beijing University of Posts and Telecommunications, Beijing 100876, China

Reprint requests to Y.-T. G.; E-mail: gaoyt@public.bta.net.cn

Z. Naturforsch. **65a**, 291–300 (2010); received April 27, 2009 / revised August 11, 2009

Under investigation in this paper, with symbolic computation, is the Sasa-Satsuma (SS) equation which can describe the propagation of ultra short pulses in optical fiber communications. By virtue of the Ablowitz-Kaup-Newell-Segur procedure, the Lax pair for the SS equation is directly established. Based on such a Lax pair, a Bäcklund transformation is constructed, through which the explicit one-soliton solution is derived. Meanwhile, an infinite number of conservation laws is provided to indicate the integrability of the SS equation in the Liouville sense. To further understand the stability of the one-soliton solution, we employ the split-step Fourier method to simulate the propagation of the soliton pulses under the finite initial perturbations. In addition, the interaction of two adjacent pulses with different separation distances is investigated through numerical simulation. Analytic and numerical results discussed in this paper are expected to be applied to the description of the optical pulse propagation.

Key words: Sasa-Satsuma Equation; Lax Pair; Bäcklund Transformation; One-Soliton Solution; Infinite Number of Conservation Laws; Soliton Interaction.

PACS numbers: 42.65.Tg, 42.81.Dp, 05.45.Yv

1. Introduction

In recent years, attention has been paid to the studies on the nonlinear evolution equations (NLEEs) [1–3] and the relevant soliton problems in the fluid dynamics [1], plasma physics [2–5], and optical fiber communications [6–10]. One of the prototype NLEEs is the nonlinear Schrödinger (NLS) equation [11–15],

$$iq_{t'} + \frac{1}{2}q_{x'x'} + |q|^2q = 0, \quad (1)$$

where q represents the complex amplitude of the pulse envelope, t' and x' are the normalized temporal and spatial variables [14]. The NLS equation usually governs the propagation of optical pulses in a monomode fiber based on the exact balance between the group velocity dispersion and self-phase

modulation [11], and the two effects lead to symmetric broadening in the time and frequency domains, respectively [16]. However, in the real fiber communications, the NLS equation becomes inadequate to describe the propagation of optical pulses in the subpicosecond or femtosecond region [13, 14]. In order to overcome the above limitations, the higher-order effects such as the third-order dispersion (TOD), self-steepening, and stimulated Raman scattering (SRS) should be considered in the NLS models [11, 12, 14, 16]. Generally speaking, those effects can produce the asymmetrical temporal broadening, asymmetrical spectral broadening, and redshift increasing in the pulse spectrum for the ultrashort pulses, respectively [16]. With that consideration, the following modified higher-order NLS (HNLS) equation has been proposed for describing the propagation of the femtosecond optical pulses in the monomode optical

fibers [11, 17],

$$\begin{aligned} & iQ_Z + \frac{1}{2}Q_{TT} + |Q|^2Q \\ & + i[\beta_1 Q_{TTT} + \beta_2 |Q|^2 Q_T + \beta_3 Q(|Q|^2)_T] \\ & = \chi[-i\Gamma Q + \sigma Q(|Q|^2)_T], \end{aligned} \quad (2)$$

where $Q(T, Z)$ is the normalized complex amplitude of the pulse envelope, Z and T represent the normalized distance along the fiber and the retarded time, respectively [17]. β_1 , β_2 , and β_3 account for the TOD, Kerr coefficient, and self-frequency shift arising from the SRS, respectively [16, 18]. The two terms on the right hand side of (2) give the fiber loss and self-induced Raman scattering effect. Moreover, Γ and σ are the real normalized parameters depending on the fiber characteristics, and χ is a small parameter [17].

Without the fiber loss and Raman scattering, i. e., when $\chi = 0$, (2) reduces to the following HNLS equation [18–20]:

$$\begin{aligned} & iQ_Z + \frac{1}{2}Q_{TT} + |Q|^2Q \\ & + i[\beta_1 Q_{TTT} + \beta_2 |Q|^2 Q_T + \beta_3 Q(|Q|^2)_T] = 0. \end{aligned} \quad (3)$$

In general, (3) is not completely integrable unless the real parameters β_1 , β_2 , and β_3 satisfy the following constraints: $\beta_1 : \beta_2 : \beta_3 = 0 : 1 : 1$, $\beta_1 : \beta_2 : \beta_3 = 0 : 1 : 0$, $\beta_1 : \beta_2 : \beta_3 = 1 : 6 : 0$, and $\beta_1 : \beta_2 : \beta_3 = 1 : 6 : 3$, which correspond to the completely integrable derivative NLS equation-type I, derivative NLS equation-type II, Hirota equation, and Sasa-Satsuma (SS) equation, respectively [13, 21–23]. In this paper, we will focus our interest on the SS equation, a generalized version of the case mentioned above [13, 20],

$$\begin{aligned} & iQ_t + \frac{1}{2}Q_{xx} + |Q|^2Q \\ & + \frac{i}{6\varepsilon}[Q_{xxx} + 6|Q|^2Q_x + 3Q(|Q|^2)_x] = 0, \end{aligned} \quad (4)$$

where Q represents a complex field, the subscripts x and t are the spatial and temporal partial derivatives, and ε is a small parameter [13, 20]. (4) can describe the development of the complex scalar field and the evolution of the short optical pulses [13, 20]. Authors of [11, 24] mention that (4) is necessary for correctly modelling the ultra-fast optical pulses in which the period of the envelope is comparable to that of the carrier, i. e., on the scale of femtoseconds. In such a situation, the pulse width can be decreased to a low level

(less than 1 ps) by the compression techniques [11], resulting in the increase of the bit rate in the optical fiber communication systems for a single carrier frequency [8].

Integrable properties of (4) have been investigated from different points of view [7, 13, 17, 20, 25, 26]. Integrability of (4) has been proved based on the inverse scattering transform (IST) method [13]. It is known that a completely integrable NLEE often admits the Bäcklund transformation (BT), Lax pair representation, Darboux transformation (DT), soliton solutions, and infinite number of conservation laws [15, 27, 28]. In addition, compared with the generalized Hirota equation [23, 29], (4) has some properties due to the different higher-order terms, which can be concluded as:

- The Lax pair is a 3×3 matrix formalization generalized from the Ablowitz-Kaup-Newell-Segur (AKNS) system [13, 30].
- The bilinearization of (4) is a reduction of the three-component Kadomtsev-Petviashvili hierarchy [31].
- The one-soliton solution derived from the IST method can exhibit the stable shape of two peaks with the same height when the specific parameters satisfy certain conditions [13].
- The types of the infinite conserved quantities for (4) are different from the ones for the Hirota equation [32].

However, we notice that most of those studies have treated the SS equation by reducing it to a complex modified Korteweg-de Vries (cmKdV) equation through the Galelian transformation, as seen in [13, 17, 20, 26, 30]. Further, integrable properties and soliton solutions have been discussed based on such a reduction [13, 17, 20, 26, 30], but the generality of the above process for (4) is inadequate to some extent, i. e., some information might be neglected [13, 31]. In fact, authors of [31] have claimed that in many previous attempts, the reduction from the SS equation to the cmKdV equation produces only rather trivial solutions, in which the complex and multicomponent freedom has been *frozen* due to the number of independent equations being more than the unknown variables. On the other hand, the two-soliton solutions have been derived analytically by virtue of the cmKdV equation [26], whereas the interaction patterns have been limited by the constraints of the real wavenumbers presented in [26].

Therefore, to better understand the features of (4), we will organize this paper, with symbolic computation [2, 3, 5, 9], as follows: In Section 2, a new Lax pair will be constructed directly from (4) by virtue of the AKNS procedure [33], which appears to be different from the one in [20]. Section 3 will present the BT by means of the Γ -Riccati form of the Lax pair. Meanwhile, the one-soliton solution of (4) will be derived via the obtained BT. In Section 4, we will construct a set of the related symmetrical Γ -Riccati equations and subsequently exhibit an infinite number of conservation laws, which are considered to be more general than the conserved quantities in [20] and [30]. In Section 5, numerical simulation for the propagation of the derived one-soliton solution under the finite initial perturbation will be investigated to demonstrate its stability. In addition, the two adjacent pulses with different separation distances will be studied on their interaction process, and the results will provide more general interaction patterns for the initial pulses, such as fusion and repulsion. Finally, our conclusions will be addressed in Section 6.

2. Lax Pair

In this section, we will employ the Painlevé analysis similar to the procedure in [18] and [34] to validate the integrability of (4) in the Painlevé sense. In order to perform the Painlevé analysis, we rewrite (4) in terms of two complex functions $q(x, t)$ and $p(x, t)$ by defining $q(x, t) = Q(x, t)$ and $p(x, t) = Q^*(x, t)$, where $*$ denotes the complex conjugate. In such case, (4) can be expressed as the following equations:

$$iq_t + \frac{1}{2}q_{xx} + q^2p + \frac{i}{6\epsilon}[q_{xxx} + 6pqq_x + 3q(pq)_x] = 0, \tag{5}$$

$$-ip_t + \frac{1}{2}p_{xx} + p^2q - \frac{i}{6\epsilon}[p_{xxx} + 6qpp_x + 3p(qp)_x] = 0. \tag{6}$$

The Weiss-Talor-Carnevale method [35] with the simplified Kruskal ansatz can be carried out to seek a solution of (5) and (6) in the form

$$q(x, t) = \varphi^{-\alpha}(x, t) \sum_{j=0}^{\infty} q_j(x, t)\varphi^j(x, t), \tag{7}$$

$$p(x, t) = \varphi^{-\beta}(x, t) \sum_{j=0}^{\infty} p_j(x, t)\varphi^j(x, t), \tag{8}$$

where $q_j(x, t)$, $p_j(x, t)$, and $\varphi(x, t)$ are the arbitrary analytic functions with variables x and t in the neighbourhood of a noncharacteristic movable singularity manifold defined by $\varphi(x, t) = 0$, while α and β are two positive integers to be determined. Via the leading order analysis, we can derive $\alpha = \beta = 1$ and $p_0q_0 = -\frac{1}{2}\varphi_x^2$. Then the resonance terms are found at $j = -1, 0, 2, 3, 4$, in which $j = -1$ corresponds to the arbitrariness of the singular manifold. Furthermore, (5) and (6) are proved to pass the Painlevé test through verifying the compatibility conditions for the remaining resonance term.

In the following content, by employing the AKNS procedure, the Lax pair for (4) can be constructed. Consider the following two linear eigenvalue problems [15]:

$$\Phi_x = U\Phi = (\lambda U_0 + U_1)\Phi, \tag{9}$$

$$\Phi_t = V\Phi = (\lambda^3 V_0 + \lambda^2 V_1 + \lambda V_2 + V_3)\Phi, \tag{10}$$

where λ is a spectral parameter, U and V are both 3×3 matrices, $\Phi = (\phi_1, \phi_2, \phi_3)^T$ with T representing the transpose of the vector. (9) and (10) are required to be compatible, so U and V should satisfy the zero curve equation,

$$U_t - V_x + [U, V] = 0, \tag{11}$$

by which the matrices U_0, U_1, V_0, V_1, V_2 , and V_3 can be determined in the following forms:

$$U_0 = \begin{pmatrix} -i & 0 & 0 \\ 0 & i & 0 \\ 0 & 0 & i \end{pmatrix}, \tag{12}$$

$$U_1 = \begin{pmatrix} 0 & kq & k^*p \\ -k^*p & 0 & 0 \\ -kq & 0 & 0 \end{pmatrix},$$

$$V_0 = \frac{2}{3\epsilon}U_0, \quad V_1 = \frac{2}{3\epsilon}U_1, \tag{13}$$

$$V_2 = \begin{pmatrix} A_1 + \frac{i}{3\epsilon}pq & kA_2 & -k^*A_2^* \\ -k^*A_2^* & A_1^* & (-k^*)^2A_3^* \\ kA_2 & k^2A_3 & A_1^* \end{pmatrix}, \tag{14}$$

$$V_3 = \begin{pmatrix} 0 & kA_4 & k^*A_4^* \\ -k^*A_4^* & A_5 & 0 \\ kA_4 & 0 & A_5^* \end{pmatrix},$$

with

$$k = \exp \left[i \left(\frac{t\varepsilon^2}{3} - x\varepsilon \right) \right], \quad A_1 = \frac{ipq}{3\varepsilon} + \frac{i\varepsilon}{2},$$

$$A_2 = \frac{q\varepsilon + iq_x}{3\varepsilon}, \quad A_3 = -\frac{iq^2}{3\varepsilon},$$

$$A_4 = -\frac{1}{6\varepsilon}(2\varepsilon^2q + 4pq^2 - 2i\varepsilon q_x + q_{xx}),$$

$$A_5 = \frac{1}{6\varepsilon}(qp_x - pq_x - 2i\varepsilon pq).$$

Substituting U and V into the compatibility condition (11), it can be proved that (11) is equivalent to (5) and its conjugate form (6). The derived Lax pair, which ensures the complete integrability of (4), can be used to construct the BT and DT to obtain the N -soliton solutions. In the next section, the one-soliton solution will be derived by employing the BT.

3. BT and One-Soliton Solution

The BT has been widely used to derive soliton solutions for the NLEEs [5, 7, 10, 35–38]. There exist several methods to obtain the BT [36], such as truncating the Painlevé expansion at the constant level term [5, 35], bilinearizing the NLEEs [37, 38], and using the Γ -Riccati form of the Lax pair [7]. Here, through the obtained Lax pair in Section 2, we can construct the BT of (4), based on which the explicit one-soliton solution can be further given as an illustrative example.

By introducing

$$\Gamma_1 = \frac{\phi_1}{\phi_3}, \quad \Gamma_2 = \frac{\phi_2}{\phi_3}, \tag{15}$$

the eigenvalue problems can be expressed in the Γ -Riccati form

$$\Gamma_{1x} = k^*p - 2i\lambda\Gamma_1 + kq\Gamma_2 + kq\Gamma_1^2, \tag{16}$$

$$\Gamma_{2x} = -k^*p\Gamma_1 + kq\Gamma_1\Gamma_2. \tag{17}$$

We can define a transformation from $(\Gamma_1, \Gamma_2, \lambda, q, p)$ to $(\Gamma'_1, \Gamma'_2, \lambda', q', p')$, which keeps the forms of (16) and (17) invariant. For simplicity, the transformation can be tried by giving $\Gamma'_1 = \Gamma_1, \Gamma'_2 = \Gamma_2$ together with $\lambda' = \lambda^*$ [7], and then the following relationships are obtained:

$$q' - q = \frac{2i\Gamma_1(\lambda^* - \lambda)}{2k\Gamma_2 + k\Gamma_1^2}, \tag{18}$$

$$p' - p = \frac{2i\Gamma_1\Gamma_2(\lambda^* - \lambda)}{2k^*\Gamma_2 + k^*\Gamma_1^2}. \tag{19}$$

(18) and (19) are regarded as the BT for (4), through which a series of explicit solutions can be obtained in a recursive manner from a given seed solution. For instance, by choosing $q_0 = 0, p_0 = 0$, and $\lambda = i\beta$ (β is a real constant), we obtain the following pseudopotentials via (16) and (17):

$$\Gamma_1 = c_1 \exp \left[2\beta x - t \left(\frac{4\beta^3}{3\varepsilon} + \beta\varepsilon \right) \right], \tag{20}$$

$$\Gamma_2 = c_2, \tag{21}$$

where c_1 and c_2 are the arbitrary complex integral constants. Furthermore, c_1 and c_2 can be found to satisfy the relationship $c_2 = c_1/c_1^*$, which implies the existence of only two arbitrary constants c_1 and β . Substituting (20) and (21) into (18) and (19), we can derive the one-soliton solution for (4), which can be expressed as

$$Q(x, t) = 4\beta c_1^* \exp \left(\frac{4t\beta^3}{3\varepsilon} + 2x\beta + t\varepsilon\beta - \frac{1}{3}it\varepsilon^2 + ix\varepsilon \right) \cdot \left[c_1 c_1^* \exp(4x\beta) + 2 \exp \left(\frac{8t\beta^3}{3\varepsilon} + 2t\varepsilon\beta \right) \right]^{-1}, \tag{22}$$

$$Q^*(x, t) = 4\beta c_1 \exp \left(\frac{4t\beta^3}{3\varepsilon} + 2x\beta + t\varepsilon\beta + \frac{1}{3}it\varepsilon^2 - ix\varepsilon \right) \cdot \left[c_1 c_1^* \exp(4x\beta) + 2 \exp \left(\frac{8t\beta^3}{3\varepsilon} + 2t\varepsilon\beta \right) \right]^{-1}. \tag{23}$$

Notice that Expression (22) can be simplified as

$$Q(x, t) = 2\beta c_1^* \exp \left(2\beta x + i\varepsilon x - \frac{i\varepsilon^2}{3}t - \frac{4\beta^3}{3\varepsilon}t - \beta\varepsilon t \right) \cdot \left[1 + \frac{|c_1|^2}{2} \exp \left(4\beta x - \frac{8\beta^3}{3\varepsilon}t - 2\beta\varepsilon t \right) \right]^{-1} \tag{24}$$

$$= \beta c_1^* \exp \left(ix\varepsilon - \frac{it\varepsilon^2}{3} - \delta \right) \cdot \operatorname{sech} \left(2x\beta - \frac{4t\beta^3}{3\varepsilon} - t\varepsilon\beta + \delta \right),$$

with $\delta = \frac{1}{2} \ln \frac{|c_1|^2}{2}$. If β and c_1 are chosen as

$$\beta = \frac{\mu}{2}, \quad c_1^* = \frac{L}{\mu}, \tag{25}$$

Expression (24) can be changed into the following form:

$$Q(x,t) = \frac{L \exp\left(\mu x + i\epsilon x - \frac{i\epsilon^2}{3}t - \frac{\mu^3}{6\epsilon}t - \frac{\epsilon\mu}{2}t\right)}{1 + \frac{|L|^2}{2\mu^2} \exp\left(2\mu x - \frac{\mu^3}{3\epsilon}t - \mu\epsilon t\right)},$$

which agrees with the result obtained by the bilinear method in [20]. Ulteriorly, other choices of β and c_1 offer a class of one-soliton solutions with similar properties.

4. Infinite Number of Conservation Laws

The rigidity in the structures of the solitons reveals that the system has a bulk underlying symmetry manifested by the existence of an infinite number of conservation laws, which provides a compelling evidence to show the integrability of (4) in the Liouville sense [30]. In this section, we will show that through the BT, not only the one-soliton solution can be derived, but also an infinite number of conservation laws can be constructed.

Firstly, we can write the auxiliary field Φ in the component form [20],

$$\Phi = \begin{pmatrix} \phi_1 \\ \phi_2 \\ \phi_3 \end{pmatrix}. \tag{26}$$

Inserting (26) into (9), the following three equations can be obtained based on the 3×3 matrices:

$$\phi_{1x} = -i\lambda\phi_1 + kq\phi_2 + k^*p\phi_3, \tag{27}$$

$$\phi_{2x} = -k^*p\phi_1 + i\lambda\phi_2, \tag{28}$$

$$\phi_{3x} = -kq\phi_1 + i\lambda\phi_3. \tag{29}$$

Defining another two associated Riccati variables in terms of $T_1 = \phi_2/\phi_1$ and $T_2 = \phi_3/\phi_1$, we derive the following two Riccati equations by eliminating T_1 and T_2 from (27)–(29):

$$T_{1x} = -k^*p + 2i\lambda T_1 - kqT_1^2 - k^*pT_1T_2, \tag{30}$$

$$T_{2x} = -kq + 2i\lambda T_2 - k^*pT_2^2 - kqT_1T_2. \tag{31}$$

In order to search for series of solutions of (30) and (31), T_1 and T_2 are assumed in the forms

$$T_1 = \sum_{n=0}^{\infty} c_n \lambda^{-n}, \tag{32}$$

$$T_2 = \sum_{n=0}^{\infty} d_n \lambda^{-n}. \tag{33}$$

Substituting the above expressions into (30), the recursion relations are given by

$$\begin{aligned} c_0 &= 0, \quad c_1 = \frac{k^*p}{2i}, \\ 2ic_{n+2} &= c_{n+1,x} \\ &+ \sum_{m=0}^{n+1} (c_m c_{n-m+1} kq + c_m d_{n-m+1} k^*p). \end{aligned} \tag{34}$$

Correspondingly, via (31), the similar recursion relations can be found as

$$\begin{aligned} d_0 &= 0, \quad d_1 = \frac{kq}{2i}, \\ 2id_{n+2} &= d_{n+1,x} \\ &+ \sum_{m=0}^{n+1} (d_m d_{n-m+1} k^*p + d_m c_{n-m+1} kq). \end{aligned} \tag{35}$$

T_1 and T_2 can be explicitly expressed by substituting the aforementioned recursion relations of c_n and d_n into Expressions (32) and (33).

Afterwards, inserting T_1 and T_2 into the equation $(\ln \phi_1)_{xt} = (\ln \phi_1)_{tx}$, an infinite number of conservation laws can be generated as [4, 39]

$$\frac{\partial D_i}{\partial t} = \frac{\partial F_i}{\partial x} \quad (i = 1, 2, \dots), \tag{36}$$

where D_i and F_i are called the conserved density and flux, respectively. Thus, the first three conserved quantities are given as:

$$\begin{aligned} D_1 &= -ipq, \\ F_1 &= \frac{ip^2q^2}{\epsilon} - \frac{p_xq}{2} + \frac{ip_{xx}q}{6\epsilon} + \frac{pq_x}{2} \\ &\quad - \frac{ip_xq_x}{6\epsilon} + \frac{ipq_{xx}}{6\epsilon}, \\ D_2 &= \frac{1}{4}(-qp_x - pq_x), \\ F_2 &= \frac{qq_xp^2}{2\epsilon} + \frac{q^2p_xp}{2\epsilon} - \frac{1}{8}iq_{xx}p + \frac{q_{xxx}p}{24\epsilon} \\ &\quad + \frac{1}{8}iqp_{xx} + \frac{qp_{xxx}}{24\epsilon}, \\ D_3 &= \frac{1}{2}ip^2q^2 - \frac{1}{4}ip\epsilon^2q - \frac{1}{4}\epsilon p_xq \\ &\quad + \frac{1}{8}ip_{xx}q + \frac{1}{8}ipq_x + \frac{1}{4}p\epsilon q_x, \end{aligned}$$

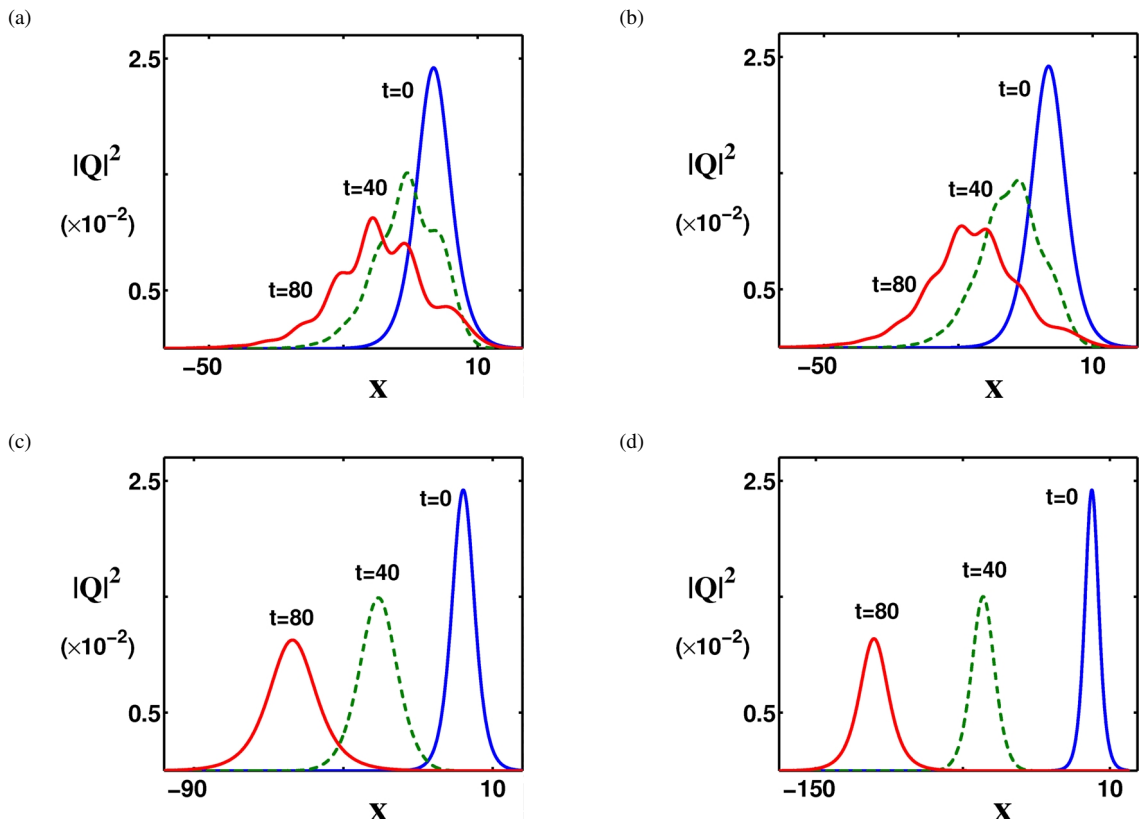


Fig. 1. Numerical simulation of the propagation of the initial pulses $Q(x,0)$ with the parameters chosen as $\beta = 0.1$ and $c_1 = 1 + i$. (a) $\epsilon = 0.17$; (b) $\epsilon = 0.2$; (c) $\epsilon = 0.5$; (d) $\epsilon = 1$.

$$\begin{aligned}
 F_3 = & -\frac{2ip^3q^3}{3\epsilon} - \frac{5ip_x^2q^2}{48\epsilon} + \frac{1}{2}ip^2\epsilon q^2 + \frac{3}{4}pp_xq^2 \\
 & - \frac{5ipp_{xx}q^2}{12\epsilon} - \frac{1}{8}\epsilon^2 p_xq + \frac{1}{6}i\epsilon p_{xx}q + \frac{5p_{xxx}q}{48} \\
 & - \frac{ip_{xxx}q}{48\epsilon} - \frac{3}{4}p^2q_xq - \frac{7ipp_xq_xq}{24\epsilon} - \frac{5ip^2q_{xx}q}{12\epsilon} \\
 & - \frac{5ip^2q_x^2}{48\epsilon} + \frac{1}{8}p\epsilon^2q_x - \frac{7}{24}i\epsilon p_xq_x \\
 & - \frac{7p_{xx}q_x}{48} + \frac{ip_{xxx}q_x}{48\epsilon} - \frac{5pq_{xx}}{48} + \frac{1}{6}ip\epsilon q_{xx} \\
 & + \frac{7p_xq_{xx}}{48} - \frac{ip_{xx}q_{xx}}{24\epsilon} + \frac{ip_xq_{xxx}}{48\epsilon} - \frac{ipq_{xxx}}{48\epsilon}. \tag{37}
 \end{aligned}$$

5. Numerical Simulation of the Pulse Propagations

In this section, we will employ the numerical simulation to analyze the propagations of the one-soliton and two adjacent solitary pulses. In details, the following two aspects will be considered: one is the propagation of Solution (24) under the finite initial

perturbation, and the other are the interactions between two adjacent pulses with the relevant parameters varying.

5.1. Stability of the One-Soliton Solution Under the Finite Initial Perturbation

Generally speaking, propagation of the soliton pulse governed by (4) is influenced by the combination of the higher-order effects such as the TOD, SS, and SRS. The balance among those effects provides the possibility for the existence of the solitons, or solitary waves, both bright and dark ones [11, 14, 40, 41]. Further, the stability of the soliton pulse under the finite initial perturbation has been commonly discussed for its theoretical and practical applications [42–44]. One notices that with the variation of the factor $1/(6\epsilon)$ in (4), different situations of the higher-order terms can be modeled. Therefore in the following content, our interest will be devoted to the propagation of Solution (24) under the finite initial perturbation (10% perturbation

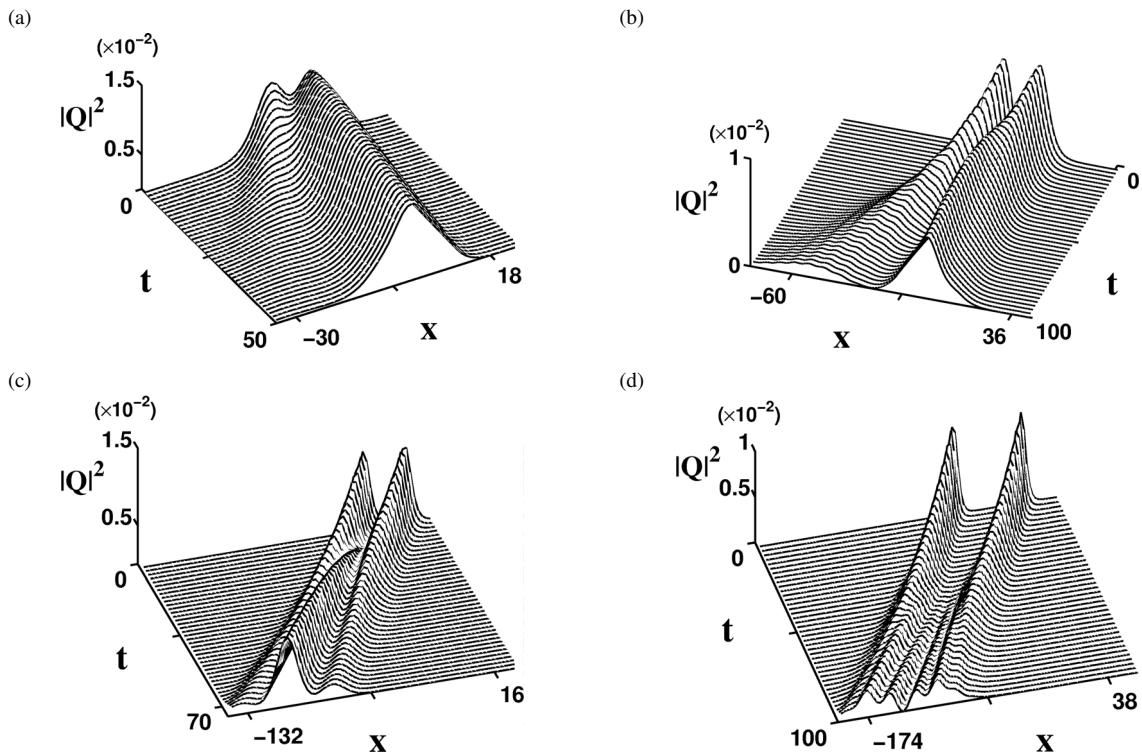


Fig. 2. Interaction of two pulses with the parameter chosen as $\beta = 0.1$. For $\epsilon = 0.17$, (a) the separation distance $T_0 = 10$; (b) $T_0 = 15$. For $\epsilon = 1$, (c) $T_0 = 25$; (d) $T_0 = 60$.

of the amplitude) with ϵ varying in the appropriate range.

Perturbed initial pulse is chosen as

$$Q(x, 0) = 1.1 \frac{\sqrt{2}\beta c_1^*}{|c_1|} \cdot \operatorname{sech} \left[2\beta x + \ln \left(\frac{|c_1|}{\sqrt{2}} \right) \right] \exp(i\epsilon x). \tag{38}$$

Numerical simulation is carried out in the MATLAB software environment by using the split-step Fourier (SSF) method [11]. The computational domain for x is chosen as $[-350, 350]$ and 7000 grid points are used. The propagation distance with respect to t is taken as 100 with a step size of 0.05. In the simulation, we accept the assumption that $0 < 1/(6\epsilon) < 1$, i.e., the range of $\epsilon > 0.167$ [26]. The parameters in the initial pulse (38) are taken as $\beta = 0.1$ and $c_1 = 1 + i$. Figures 1a–d present the numerical results with ϵ increasing, which demonstrate that the perturbed initial pulses propagate in different manners depending on the choices of ϵ . When the value of ϵ is small, the initial pulse is distorted such that it becomes asymmetric with

several humps emerging (see Fig. 1a) and the pulse broadening is remarkable for the long time propagation. On the other hand, the higher-order effects, such as the TOD, which can make the intensity amplitude asymmetric and introduce a long oscillating tail [11], will contribute to the stability of the pulse propagation as the factor $1/(6\epsilon)$ is not small. As ϵ increases, the shape of perturbed pulse tends to be smooth and exhibits only the broadening effect (see Figs. 1b–d). Further, the perturbed pulse seems to acquire an increasing velocity along the x propagation direction as ϵ growing. For a larger value of ϵ , the influence of the higher-order effects is weakening and the pulse can propagate more stably (with weaker broadening) within the same distance along x .

5.2. Interaction Between Two Adjacent Pulses

For the models governed by the NLS-typed equations, the interaction between the two adjacent initial pulses have attracted considerable interest [41, 43–47]. Those interactions include a variety of patterns, such as the periodic merger and separation, re-

pulsion and fusion, depending on the initial conditions to some extent [43, 45]. In this section, the two adjacent pulses with different separation distances and relevant parameters will be studied on their interaction process through numerical simulation. Although the analytic expression of the two-soliton solutions for (4) exist [26], it requires the two wavenumbers to be real and satisfy an exact dispersion relation, which is not generic enough in generating the initial pulses in the optical fiber communications. Here the initial pulse can be given as

$$Q(x, 0) = \beta \operatorname{sech} \left[2\beta \left(x + \frac{T_0}{2} \right) \right] \exp \left[i\epsilon \left(x + \frac{T_0}{2} \right) \right] + \beta \operatorname{sech} \left[2\beta \left(x - \frac{T_0}{2} \right) \right] \exp \left[i\epsilon \left(x - \frac{T_0}{2} \right) \right], \quad (39)$$

where T_0 is the initial separation distance of the two pulses with respect to x , β and ϵ are the parameters introduced in Solution (24) and (4), respectively. The above form of the pulse is based on the analytic Solution (24), but convenient and general for the numerical simulation.

Results with the typical values of ϵ are demonstrated in Figure 2 for the separation distances $T_0 = 10, 15, 25$, and 60. In the case of $\epsilon = 0.17$, most of the two initial pulses are overlapped for $T_0 = 10$ and the pulses interact asymmetrically with t propagating (see Fig. 2a). The amplitude of one pulse exhibits gradually attenuation and its energy is transformed to the coherent pulse, the width of which is induced to broaden during the 100 propagating distance with respect to t . When $T_0 = 15$, the similar attenuation and broadening for each pulse exist in like manner, however, the two pulses repel each other at the propagating distance of approximately 40 and the left pulse appears to propagate parallel to axis t (see Fig. 2b). For $\epsilon = 1$, the pulse interactions for $T_0 = 10$ and 15 are analogous to those in Figures 2a and b, but the repulsion for $T_0 = 15$ is not visible. Figures 2c and d present the interactions for larger separation distances $T_0 = 25$ and 60 in the case of $\epsilon = 1$. When $T_0 = 25$, the two solitary pulses begin to evolve into one pulse whose amplitude increases promptly after about 25 propagating distance, and at the same time, the two initial pulses attenuate with the width broadening (see Fig. 2c). The numerical calculation for $\epsilon = 0.17$ reveals that the fusion-like interaction occurs for $T_0 = 35 \sim 40$, but some small oscillations exist on the

file surface, which can be viewed as the similar effect to that in Figure 1a. When $T_0 = 60$, the two pulses can propagate for a longer distance along t , exhibiting the width broadening before their interaction. After about 75 propagating distance, the multi-hump structure is formed through the interaction (see Fig. 2d), and such humps are more disordered in the case of $\epsilon = 0.17$.

Therefore, one notices that due to the combined effects of the TOD, self-steepening, and SRS, the interactions between the two adjacent pulses have certain features similar to those in the propagation of the one-soliton solution under finite initial perturbation, such as the pulse broadening and formation of the multi-hump structures. Considering that, the analytic solutions need some strict balances and restrains among the terms in (4) and relevant parameters, respectively, which would be difficult to produce, the above numerical simulation might provide some necessary information for the understanding of the propagation and interaction of the solitary pulses.

6. Conclusions

In this paper, considering the role of the SS equation, i. e., Equation (4), in describing the evolution of ultra short pulses, which can benefit the high capacity transmission in the optical fiber communications, we have investigated the SS equation from the integrable point of view. Following the AKNS procedure, we have constructed the 3×3 matrix Lax pair and further obtained the BT. Based on the BT, the one-soliton solution has been derived, which can be viewed as the generalized form of the one obtained by the bilinear method under certain parametric conditions. In addition, by the symmetrical Riccati equations, an infinite number of conservation laws have been presented, as a proof of the integrability in the Liouville sense. Furthermore, propagation of the one-soliton pulse under the finite initial perturbation has been analyzed with the SSF method. Synchronously, interaction processes of the two adjacent pulses with different separation distances and relevant parameters have been studied through numerical simulation. It is expected that the analytic results discussed in this paper would be helpful in studying the linear eigenvalue problems with the 3×3 matrix and similar integrable properties of the models in optical fiber communications. Meanwhile, numerical simulation for the propagation of the one-

soliton and two adjacent solitary pulses could provide certain applications in those nonlinear optical fields.

On the other hand, the coupled HNLS (CHNLS) equations have been derived from the vector form of (4) with \vec{Q} as a sum of the left- and right-handed polarized waves [18], which have the relevant applications in the electromagnetic pulse propagations in the coupled optical waveguides and in a weakly relativistic plasma with the nonlinear coupling of two polarized transverse waves [18]. Considering the similarities between (4) and the coupled ones, the same analytic and numerical procedures can be addressed to discuss the relevant integrable properties for the CHNLS equations.

Acknowledgements

We express our sincere thanks to all the members of our discussion group for their valuable comments. This work has been supported by the National Natural Science Foundation of China under Grant No. 60772023, by the Open Fund of the State Key Laboratory of Software Development Environment under Grant No. BUAA-SKLSDE-09KF-04, Beijing University of Aeronautics and Astronautics, by the National Basic Research Program of China (973 Program) under Grant No. 2005CB321901 and by the Specialized Research Fund for the Doctoral Program of Higher Education (Nos. 20060006024 and 200800130006), Chinese Ministry of Education.

- [1] Y.S. Kachanov, O.S. Ryzhov, and F.T. Smith, *J. Fluid Mech.* **251**, 273 (1993); K.W. Chow, N.W. Ko, R.C. Leung, and S.K. Tang, *Phys. Fluids* **10**, 1111 (1998).
- [2] M.P. Barnett, J.F. Capitani, J. von zur Gathen, and J. Gerhard, *Int. J. Quantum Chem.* **100**, 80 (2004); W.P. Hong, *Phys. Lett. A* **361**, 520 (2007); B. Tian and Y.T. Gao, *Phys. Lett. A* **340**, 243 (2005); **362**, 283 (2007).
- [3] G. Das and J. Sarma, *Phys. Plasmas* **6**, 4394 (1999); Y.T. Gao and B. Tian, *Phys. Lett. A* **349**, 314 (2006); *Phys. Plasmas* **13**, 112901 (2006); *Phys. Plasmas (Lett.)* **13**, 120703 (2006); *Europhys. Lett.* **77**, 15001 (2007).
- [4] T. Xu, B. Tian, L.L. Li, X. Lü, and C. Zhang, *Phys. Plasmas* **15**, 102307 (2008).
- [5] B. Tian and Y.T. Gao, *Phys. Plasmas (Lett.)* **12**, 070703 (2005); *Eur. Phys. J. D* **33**, 59 (2005); Y.T. Gao and B. Tian, *Phys. Lett. A* **361**, 523 (2007).
- [6] Y. Kivshar and G.P. Agrawal, *Optical Solitons, From Fibers to Photonic Crystals*, Academic Press, New York 2003.
- [7] K. Nakkeeran, K. Porsezian, P.S. Sundaram, and A. Mahalingam, *Phys. Rev. Lett.* **80**, 1425 (1998).
- [8] T. Brugarino and M. Sciacca, *Opt. Commun.* **262**, 250 (2006).
- [9] B. Tian, W.R. Shan, C.Y. Zhang, G.M. Wei, and Y.T. Gao, *Eur. Phys. J. B (Rapid Not.)* **47**, 329 (2005); B. Tian and Y.T. Gao, *Phys. Lett. A* **342**, 228 (2005); **359**, 241 (2006).
- [10] B. Tian, Y.T. Gao, and H.W. Zhu, *Phys. Lett. A* **366**, 223 (2007); W.J. Liu, B. Tian, H.Q. Zhang, L.L. Li and Y.S. Xue, *Phys. Rev. E* **77**, 066605 (2008); W.J. Liu, B. Tian, and H.Q. Zhang, *Phys. Rev. E* **78**, 066613 (2008).
- [11] G.P. Agrawal, *Nonlinear Fiber Optics*, 3rd ed., Academic Press, San Diego 2001.
- [12] A. Hasegawa and F.D. Tappert, *Appl. Phys. Lett.* **23**, 142 (1973); L.F. Mollenauer, R.H. Stolen, and J.P. Gordon, *Phys. Rev. Lett.* **45**, 1095 (1980).
- [13] N. Sasa and J. Satsuma, *J. Phys. Soc. Jpn.* **60**, 409 (1991).
- [14] A. Mahalingam and K. Porsezian, *Phys. Rev. E* **64**, 046608 (2001).
- [15] J. Li, H.Q. Zhang, T. Xu, Y.X. Zhang, and B. Tian, *J. Phys. A* **40**, 13299 (2007).
- [16] Z.H. Li, L. Li, H.P. Tian, and G.S. Zhou, *Phys. Rev. Lett.* **84**, 4096 (2000).
- [17] D. Mihalache, L. Torner, F. Moldoveanu, N.C. Panoiu, and N. Truta, *Phys. Rev. E* **48**, 4699 (1993).
- [18] K. Porsezian, P. Shanmugha Sundaram, and A. Mahalingam, *Phys. Rev. E* **50**, 1543 (1994).
- [19] Y. Kodama and A. Hasegawa, *Phys. Rev. E* **23**, 510 (1987).
- [20] S. Ghosh, A. Kundu, and S. Nandy, *J. Math. Phys.* **40**, 1993 (1999).
- [21] D. Anderson and M. Lisak, *Phys. Rev. A* **27**, 1393 (1983).
- [22] H.H. Chen, Y.C. Lee, and C.S. Liu, *Phys. Scr.* **20**, 490 (1979).
- [23] R. Hirota, *J. Math. Phys.* **14**, 805 (1973).
- [24] A. Hasegawa and Y. Kodama, *Solitons in Optical Communications*, Clarendon Press, Oxford 1995.
- [25] K. Porsezian, P. Shanmugha Sundaram, and A. Mahalingam, *J. Phys. A* **32**, 8731 (1999).
- [26] M. Daniel and M.M. Latha, *Physica A* **298**, 351 (2001).
- [27] M.J. Ablowitz and P.A. Clarkson, *Solitons, Nonlinear Evolution Equations, Inverse Scattering*, Cambridge University Press, Cambridge 1991.

- [28] P. A. Clarkson, *IMA J. Appl. Math.* **44**, 27 (1990).
- [29] K. Porsezian, *J. Phys. A* **24**, L337 (1991).
- [30] S. Ghosh and S. Nandy, *Nucl. Phys. B* **561**, 451 (1999).
- [31] C. Gilson, J. Hietarinta, J. Nimmo, and Y. Ohta, *Phys. Rev. E* **68**, 016614 (2003).
- [32] J. Kim, Q. H. Park, and H. J. Shin, *Phys. Rev. E* **58**, 6746 (1998).
- [33] M. J. Ablowitz, D. J. Kaup, A. C. Newell, and H. Segur, *Phys. Rev. Lett.* **31**, 125 (1973).
- [34] D. Mihalache, N. Truta, and L. C. Crasovan, *Phys. Rev. E* **56**, 1064 (1997).
- [35] J. Weiss, M. Tabor, and G. Carnevale, *J. Math. Phys.* **24**, 522 (1983).
- [36] C. Y. Zhang, Y. T. Gao, T. Xu, L. L. Li, F. W. Sun, J. Li, X. H. Meng, and G. M. Wei, *Commun. Theor. Phys.* **49**, 673 (2008).
- [37] X. Lü, H. W. Zhu, X. H. Meng, Z. C. Yang, and B. Tian, *J. Math. Anal. Appl.* **336**, 1305 (2007).
- [38] X. H. Meng, B. Tian, T. Xu, H. Q. Zhang, and Q. Feng, *Phys. A* **388**, 209 (2009).
- [39] M. Wadati, H. Sanuki, and K. Konno, *Prog. Theor. Phys.* **53**, 419 (1975).
- [40] H. P. Tian, Z. H. Li, and G. S. Zhou, *Opt. Commun.* **205**, 221 (2002).
- [41] J. P. Tian, and G. S. Zhou, *Phys. Scr.* **73**, 56 (2006).
- [42] X. J. Shi, L. Li, R. Y. Hao, Z. H. Li, and G. S. Zhou, *Opt. Commun.* **241**, 185 (2004).
- [43] R. Grimshaw, K. Nakkeeran, C. K. Poon, and K. W. Chow, *Phys. Scr.* **75**, 620 (2007).
- [44] F. Fang and Y. Xiao, *Opt. Commun.* **268**, 305 (2006).
- [45] G. I. Stegeman and M. Segev, *Sci.* **286**, 1518 (1999).
- [46] T. Kanna, M. Lakshmanan, P. T. Dinda, and N. Akhmediev, *Phys. Rev. E* **73**, 026604 (2006).
- [47] J. Yang, *Phys. Rev. E* **64**, 026607 (2001).